© 2018. Published by The Company of Biologists Ltd | Journal of Cell Science (2018) 131, jcs221457. doi:10.1242/jcs.221457

RESEARCH ARTICLE

The RHEB–mTOR axis regulates expression of *Tf2* transposons in fission yeast

Yukiko Nakase[1] and Tomohiro Matsumoto[1,2,*]

ABSTRACT

The human *TSC2* gene, mutations in which predispose individuals to the disease tuberous sclerosis complex (TSC), encodes a GTPase-activating protein for the GTPase RHEB. Loss of TSC2 results in constitutive activation of RHEB and its target mammalian target of rapamycin (mTOR). We have previously reported that fission yeast (*Schizosaccharomyces pombe*) *Tf2* retrotransposons (hereafter *Tf2*s) are abnormally induced upon nitrogen starvation in cells lacking the *tsc2*$^{+}$ gene (*Δtsc2*), a homolog of the human *TSC2* gene, and in cells with a dominant-active mutation in the fission yeast RHEB GTPase (*rhb1-DA4*). We report here that induction of *Tf2*s in these mutants is suppressed upon overexpression of the *cgs2*$^{+}$ gene, which encodes a cAMP-specific phosphodiesterase, or upon deletion of components in the glucose/cAMP signaling pathway, namely Cyr1, Pka1, Tor1 and the stress-activated transcription factor Atf1. The results suggest that the glucose/cAMP signaling pathway is downregulated when cells are starved for nitrogen. We also show that Tf2 proteins are degraded via autophagy, which is under control of Tor2, a homolog of human mTOR. It appears that failure in the two processes, downregulation of the glucose/cAMP signaling pathway and induction of autophagy, allows abnormal induction of *Tf2*s upon nitrogen starvation in *Δtsc2* and *rhb1-DA4* cells.

KEY WORDS: Tuberous sclerosis complex, RHEB–mTOR, Transposon, Nitrogen starvation, Glucose/cAMP signaling, Autophagy

INTRODUCTION

Transposable elements (TEs) were first reported as DNA sequences that can move from one location to another in the genome (McClintock, 1950). They are found in both prokaryotes and eukaryotes, and make up ∼50% of the human genome and up to 90% of the maize genome (SanMiguel et al., 1996). Depending on the intermediate required for mobilization, TEs are categorized into two groups, retrotransposons (class I) and DNA transposons (class II). Class I TEs are first transcribed from DNA to RNA by a reverse transcriptase, which is often encoded by the TE itself. The RNA produced is then transcribed to DNA, which is inserted back into the genome. Transposition of Class II TEs, which does not involve an RNA intermediate, is catalyzed by several enzymes (transposases). The transposase makes a cut at the target site in the genome, producing sticky ends, then cuts out the DNA transposon and ligates it into the target site.

In order to maintain the genome integrity, expression of TEs are normally suppressed by the host mechanisms. Expression of retrotransposons is suppressed by DNA methylation in mammals (Crichton et al., 2014; Li et al., 2015). Recent studies also have suggested that histone methylation plays a role as a suppressor in human and mouse (Hutnick et al., 2010; Leung and Lorincz, 2012). RNA interference (RNAi) is an additional mechanism to suppress expression of TEs in various organisms (Dumesic and Madhani, 2014). While expression and propagation of TEs are considered to be harmful for the host genome, TEs, when induced by stresses, serve as a useful source for the creation of new genetic variability, which consequently helps the host organisms adapt to stresses (Capy et al., 2000). Interestingly, TEs are abundantly expressed in mammalian oocytes and early embryos (Evsikov et al., 2006; Peaston et al., 2004). It has been shown that TEs play critical roles in gene regulation for the specification of cell types in early mammalian development (Macfarlan et al., 2012). Furthermore, TEs are active in developing neurons (Muotri et al., 2005) and in the adult brain (Baillie et al., 2011), resulting in mosaicism whereby cells within an individual have a different genetic makeup. These findings strongly suggest that TEs do not act as simple parasitic sequences, but have co-evolved with the host organisms.

In the fission yeast *Schizosaccharomyces pombe*, the *Tf2* element is a class I TE with a genome of 4.9 kb (Hoff et al., 1998). The genome of fission yeast contains only 13 copies of *Tf2* occupying less than 0.5% of the genome, suggesting that propagation/amplification of the *Tf2* retrotransposons (hereafter denoted *Tf2*s) has been highly restricted in this organism.

We have previously shown that, upon nitrogen starvation, *Tf2*s are abundantly induced in cells lacking the *tsc1*$^{+}$ or *tsc2*$^{+}$ gene, a fission yeast homolog of human genes *TSC1* or *TSC2* (Nakase et al., 2006). Mutations in the human genes *TSC1* and *TSC2* predispose individuals to the disease tuberous sclerosis complex (TSC), which is characterized by widespread development of benign tumors called hamartomas (European Chromosome 16 Tuberous Sclerosis Consortium, 1993; Kwiatkowski and Short, 1994; van Slegtenhorst et al., 1997). TSC1 and TSC2 proteins form a heterodimer and control cell growth/proliferation by regulating the activity of the small GTPase RHEB (Garami et al., 2003; Inoki et al., 2002; Manning and Cantley, 2003). When the environment is not favorable for growth/proliferation, the TSC1–TSC2 complex converts RHEB into an inactive form by stimulating hydrolysis of GTP bound to RHEB. Mammalian target of rapamycin (mTOR) is a major target of RHEB and promotes protein synthesis for cell proliferation when stimulated by the RHEB GTPase (Fingar and Blenis, 2004; Raught et al., 2001). Functional loss of TSC1 or TSC2 therefore leads to prolonged activation of RHEB and its target mTOR. We and other groups have shown that fission yeast Tsc1 and Tsc2 regulate Rhb1, a homolog of RHEB, which, in turn, targets

[1]Radiation Biology Center, Kyoto University, Yoshida-Konoe cho, Sakyo ku, Kyoto 606-8501, Japan. [2]Graduate School of Biostudies, Kyoto University, Yoshida-Konoe cho, Sakyo ku, Kyoto 606-8501, Japan.

*Author for correspondence (tmatsumo@house.rbc.kyoto-u.ac.jp)

Y.N., 0000-0002-2669-5539; T.M., 0000-0001-6199-5126

Received 11 June 2018; Accepted 1 October 2018

Journal of Cell Science (2018) 131, jcs221457. doi:10.1242/jcs.221457

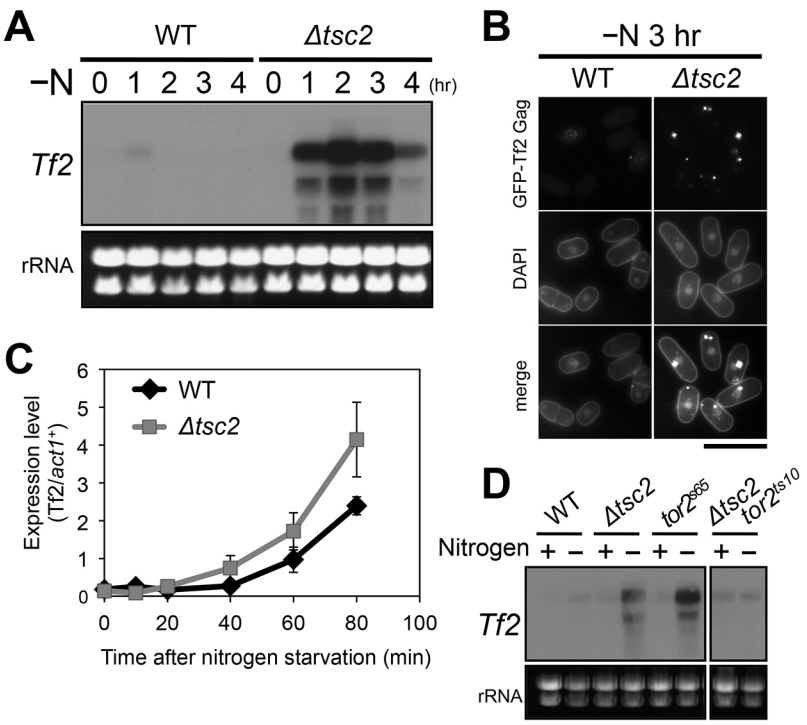

Fig. 1. Expression of *Tf2* retrotransposons in *Δtsc2* under nitrogen starvation. (A) *Tf2*s are excessively expressed in *Δtsc2*. WT and *Δtsc2* cells were pre-cultured overnight in nitrogen-rich medium containing 3% glucose (EMM+N) and then transferred to nitrogen-poor medium containing 3% glucose (EMM−N). Total RNAs were analyzed by northern blot hybridization with *Tf2* as a probe. (B) The GFP-tagged retrotransposon gene Gag localizes as distinct dots in the cytoplasm. Cells were cultured as in A. The *Tf2-13* gene was tagged with GFP and chromosomally integrated for expression from the native promoter. GFP–Tf2 Gag formed virus-like particles (VLPs) in *Δtsc2* cells 3 h after nitrogen starvation. Scale bar:10 µm. (C) *Tf2*s are induced earlier in *Δtsc2* cells than in WT cells. Cells were cultured and collected as in A. *Tf2* RNA levels were analyzed by qRT-PCR. Data are presented as mean±s.e.m. (*n*=3). (D) *Tf2*s are excessively expressed in the Tor2 active mutant *tor2*^{s65}, but are suppressed in the Tor2 loss-of-function mutant *tor2*^{ts10}. Cells were treated and analyzed as in A. +, nitrogen rich; −, 2.5 h after nitrogen starvation.

Tor2 in fission yeast, a homolog of mTOR (Mach et al., 2000; Matsumoto et al., 2002; Matsuo et al., 2007; van Slegtenhorst et al., 2004). When the environment is favorable for proliferation, active Tor2 stimulates protein synthesis and suppresses the onset of meiosis.

In this study, we have attempted to understand the underlying mechanism that allows abnormal induction of *Tf2*s upon nitrogen starvation in cells lacking the *tsc2*$^{+}$ gene (*Δtsc2*). Through a genetic screen for a suppressor of *Δtsc2*, we have identified the *cgs2*$^{+}$ gene, which encodes a cAMP-specific phosphodiesterase that is known to act as a regulator in the glucose/cAMP signaling pathway (Matviw et al., 1993). Consistently, deletion of components in the glucose/cAMP signaling pathway, namely Cyr1, Pka1 and Tor1, also suppresses the abnormal induction of *Tf2*s seen in both *Δtsc2* cells and cells that have dominant-active mutation in the Rhb1 GTPase (*rhb1-DA4*). These results suggest that the glucose/cAMP signaling pathway is downregulated when cells are starved for nitrogen. We also show that *Tf2*s are degraded via autophagy, which is under control of Tor2, a homolog of human mTOR. Failure in the two processes, downregulation of the glucose/cAMP signaling pathway

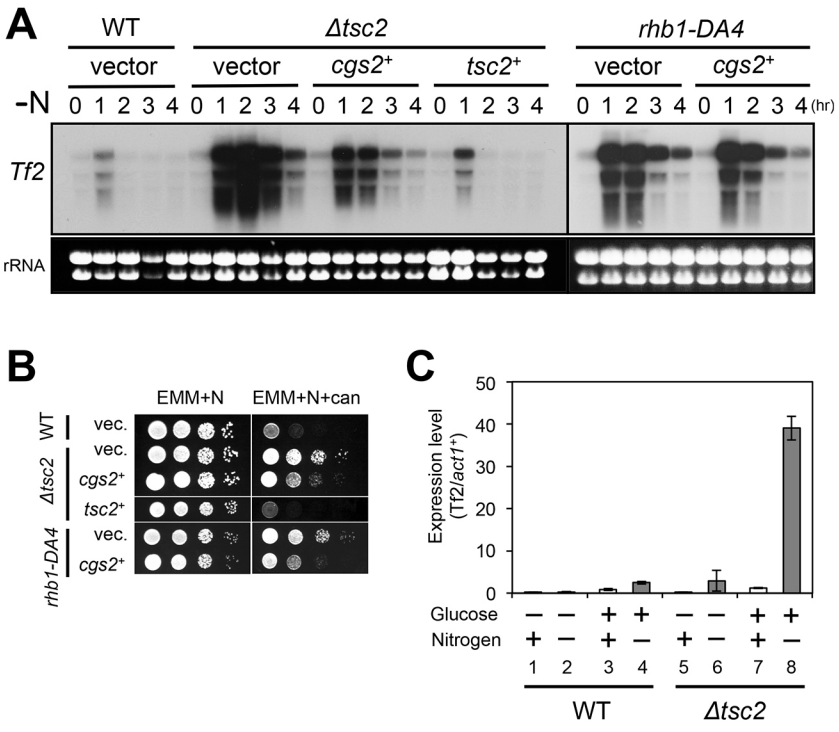

Fig. 2. Involvement of glucose/cAMP signaling pathway in expression of *Tf2*s. (A) *cgs2+* is a multicopy suppressor of *Δtsc2* mutant. Cells were transformed with pAL-KS vector, or plasmids expressing *cgs2*$^{+}$ or *tsc2*$^{+}$. Transformants were treated and analyzed as in Fig. 1A. (B) *cgs2*$^{+}$ partially suppresses the resistance of *Δtsc2* and *rhb1-DA4* strains to canavanine. Transformants were suspended in liquid EMM at a concentration of 10^{7} cells/ml, and 5 µl of the suspension was spotted onto an EMM+N plate (left) or EMM+N containing canavanine (60 mg/ml; right). They were incubated for 3 days at 30°C. (C) *Tf2*s are not induced under glucose starvation. Lanes 1 and 5, cells were grown to mid-log phase in nitrogen-rich medium containing 3% glucose and then transferred onto glucose-depleted medium (0.1% glucose) for 6 h. Lanes 2 and 6, cells were cultured as for lanes 1 and 5. After that, cells were shifted to nitrogen-poor and glucose-depleted medium for 2 h. Lanes 3 and 7, cells were grown to mid-log phase in nitrogen-rich medium containing 3% glucose. Lanes 4 and 8, cells were cultured as for lanes 3 and 7. After that, cells were shifted to nitrogen-poor medium containing 3% glucose for 2 h. *Tf2* mRNA levels were analyzed by qRT-PCR. Data are presented as mean±s.e.m. (*n*=3)

Journal of Cell Science (2018) 131, jcs221457. doi:10.1242/jcs.221457

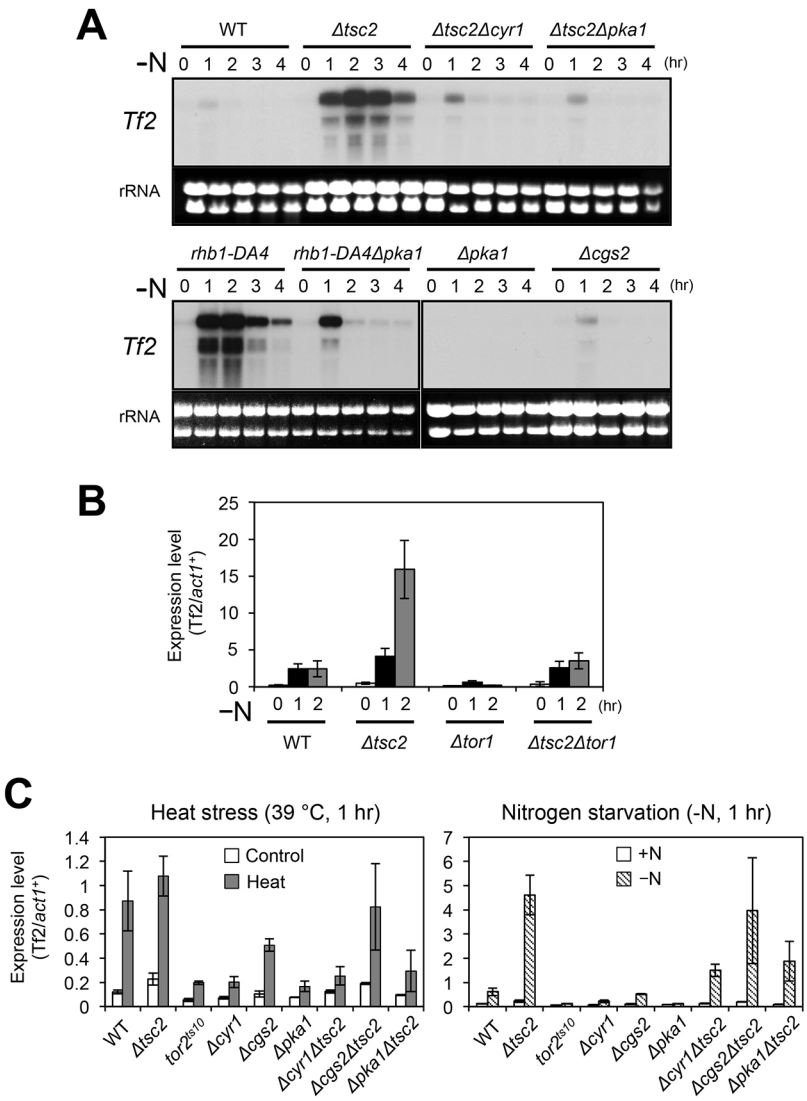

Fig. 3. Contribution of glucose/cAMP signaling pathway to expression of *Tf2*s in response to various stresses. (A) *Δpka1* and *Δcyr1* suppresses expression of *Tf2*s in *Δtsc2* and *rhb1-DA4* cells. Cells were treated and analyzed as in Fig. 1A. (B) *Δtor1* suppresses expression of *Tf2*s in the *Δtsc2* mutant. Cells were treated and analyzed as in Fig. 1C. (C) Heat stress cause expression of *Tf2*s. Cells were grown to mid-log phase in nitrogen-rich medium containing 3% glucose (Stephan et al., 2009) at 26°C and then shifted to 39°C for 1 h (left) or to EMM–N for 1 h (right). Tf2 RNA levels were analyzed by qRT-PCR. Data are presented as mean±s.e.m. (*n*=3).

and induction of autophagy, allows abnormal induction of *Tf2*s upon nitrogen starvation in *Δtsc2* and *rhb1-DA4* cells. Our study has revealed a novel role of the RHEB–mTOR axis in regulation of expression of *Tf2*s, which may contribute to adaptation to the nutrient stress and/or protection of the integrity of the genome.

RESULTS

Expression of *Tf2* retrotransposons upon nitrogen starvation

We have previously shown that *Tf2* retrotransposon genes were abundantly expressed in mutants null for *tsc1* or *tsc2* (*Δtsc1* or *Δtsc2*) under nitrogen-poor conditions (Nakase et al., 2006). As shown in Fig. 1A, *Tf2*s were rapidly induced and the level of expression reached a peak 2–3 h after nitrogen starvation in *Δtsc2* cells. We examined the timing of the induction of *Tf2*s in detail. *Tf2*s were induced ∼40 min after nitrogen starvation in wild-type (WT) cells and they were induced faster in *Δtsc2* cells, by ∼10 min (Fig. 1C). Using fluorescence microscopy, we observed the expression and localization of the GFP-tagged retrotransposon gene *gag* encoding the capsid protein. Gag forms virus-like particles (VLPs) including retrotransposon mRNAs, reverse transcriptase and integrase, which are required for integration into the host genome (Swanstrom and Wills, 1997). Gag proteins tagged with GFP localized as distinct dots in the cytoplasm after nitrogen starvation and the fluorescence intensity of GFP was stronger in *Δtsc2* cells than in WT cells (Fig. 1B).

Tor2, which is a member of the TORC1 complex, is regulated by Tsc1/2 (Weisman et al., 2007). In *Δtsc2* cells, Tor2 is constitutively activated and prevents induction of the *mei2*$^{+}$ gene after nitrogen starvation (Nakase et al., 2006). In cells expressing the dominant-active Tor2 mutant *tor2*^{s65}, *Tf2*s were significantly expressed after nitrogen starvation. Expression of the temperature-sensitive Tor2 mutant *tor2*^{ts10}, which causes a partial loss of function, suppressed expression of *Tf2*s in *Δtsc2* cells (Fig. 1D). These results suggested that Tor2 plays a key role in regulation of *Tf2*s expression after nitrogen starvation.

Glucose/cAMP signaling regulates *Tf2*s expression

In order to reveal the underlying mechanism(s) to allow induction of *Tf2*s in *Δtsc2*, we attempted to isolate and characterize a multicopy suppressor of *Δtsc2*. As we previously reported (Nakase et al., 2013), a loss of *tsc2*$^{+}$ caused defective uptake of a variety of amino acids, including arginine, and, thereby, conferred resistance to canavanine, a toxic analog of arginine. By selecting and subcloning a plasmid in a fission yeast genomic DNA library that was able to reverse the resistance to canavanine, we identified the *cgs2*$^{+}$ gene, which encodes a cAMP phosphodiesterase (PDE). As shown in

Journal of Cell Science (2018) 131, jcs221457. doi:10.1242/jcs.221457

Fig. 2B, overexpression of *cgs2*$^+$ partially suppressed the resistance to canavanine of *Δtsc2*. It also partially suppressed expression of *Tf2*s (Fig. 2A). We previously reported that *Tf2*s were induced in the *rhb1-DA4* mutant, which is a dominant-active mutant of the Rhb1 GTPase (Murai et al., 2009). Overexpression of *cgs2*$^+$ also partially suppressed expression of *Tf2*s in the *rhb1-DA4* mutant (Fig. 2A).

Because Cgs2 was best known as a negative regulator of the intracellular cAMP level in a feedback control of glucose/cAMP signaling (Wang et al., 2005), we tested the effect of glucose starvation on expression of *Tf2*s. Cells grown to mid-log phase in nitrogen-rich medium containing 3% glucose were transferred to glucose-depleted medium (0.1% glucose) for 6 h. As shown in Fig. 2C (lanes 1 and 5), no apparent expression of *Tf2*s was observed in WT or *Δtsc2* cells. When these glucose-starved cells were further shifted to glucose-depleted and nitrogen-poor medium, weak induction of *Tf2*s was observed in *Δtsc2* (lane 6). The results indicated that depletion of glucose did not induce expression of *Tf2*s.

We next examined the genetic interaction between *Δtsc2* and deletion mutants of other components in the glucose/cAMP signaling pathway, namely Cyr1, Pka1 and Tor1. By producing cAMP, Cyr1 activates the cAMP-dependent protein kinase Pka1 (Welton and Hoffman, 2000). Cgs2 antagonizes Cyr1 by converting cAMP into AMP (Matviw et al., 1993). Because overexpression of Cgs2 suppressed the induction of *Tf2*s in *Δtsc2*, we expected that deletion of *cyr1*$^+$ would also suppress the induction. As shown in Fig. 3A, the level of expression of *Tf2*s was dramatically reduced in the double mutant *Δtsc2 Δcyr1*. Likewise, deletion of *pka1*$^+$ suppressed the induction of *Tf2*s in *Δtsc2* and *rhb1-DA4* cells. Overexpression of *pka1*$^+$, on the other hand, resulted in induction of *Tf2*s in the WT strain starved for nitrogen (Fig. S1A). Because Atf1 is a stress-activated transcription factor under control of Pka1 (Kanoh et al., 1996), we suspected that Atf1 was responsible for transactivation of *Tf2*s. As shown in Fig. S1B, the expression level of *Tf2*s upon nitrogen starvation decreases in the double mutant *Δatf1 Δtsc2*. The level of *Tf2*s in *Δpka1 Δtsc2* was lower than that in *Δatf1 Δtsc2*, suggesting that Pka1 might also control other transcription factors, such as Atf21 and Atf31 (Mata et al., 2007), to mediate transactivation of *Tf2*s.

Tor1, which forms the TORC2 complex with Ste20, Sin1 and Wat1 (Matsuo et al., 2007), is required for survival under stress conditions (Kawai et al., 2001; Weisman and Choder, 2001). It was reported that the glucose/cAMP signaling pathway activates TORC2 and its downstream element, Gad8 (Cohen et al., 2014). We found that *Δtor1* could suppress expression of *Tf2*s in *Δtsc2* after nitrogen starvation (Fig. 3B).

We also examined the contribution of the components in the glucose/cAMP signaling pathway to induction of *Tf2*s in response to heat shock. As shown in Fig. 3C, Cyr1 and Pka1 were required for efficient induction of *Tf2*s upon heat shock. These results suggested that the glucose/cAMP signaling pathway is involved in *Tf2*s expression upon nitrogen starvation as well as heat shock.

The glucose/cAMP signaling pathway in *Δtsc2* cells

The results described above suggested that a culprit for abnormal induction of *Tf2*s in *Δtsc2* was the glucose/cAMP signaling pathway, which was continuously upregulated by the RHEB–mTOR axis. We analyzed the glucose/cAMP signaling pathway biochemically to determine a component targeted by RHEB–mTOR axis. We first measured the level of cAMP upon nitrogen starvation. As shown in Fig. S2A, the level of cAMP at 1 h after nitrogen starvation dropped

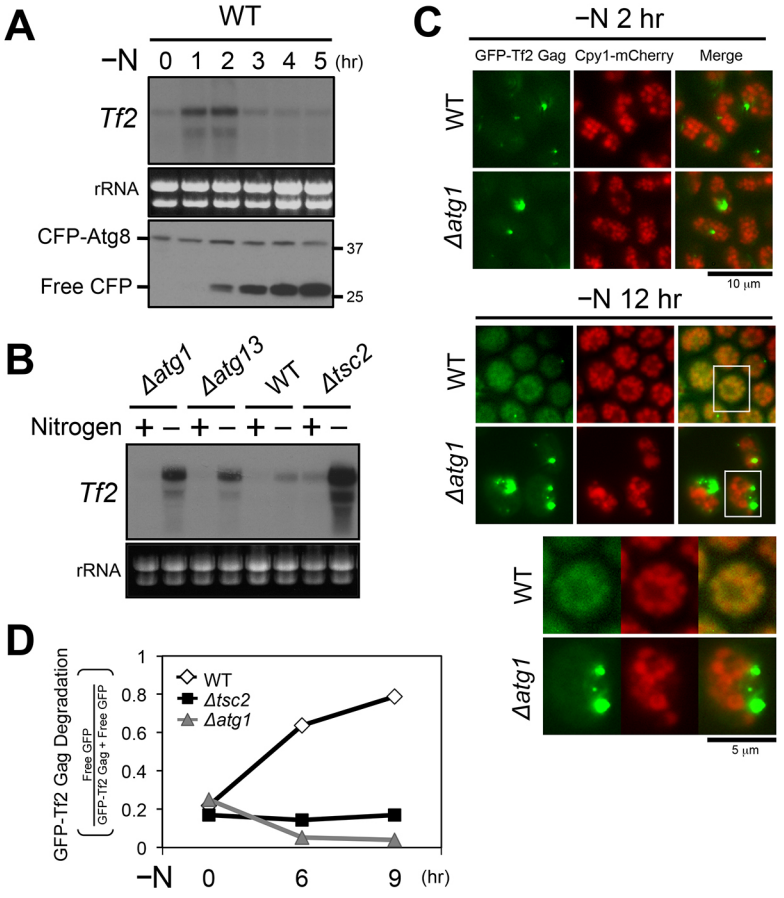

Fig. 4. Degradation of Tf2-containing VLPs by autophagy. (A) The timing of autophagy and expression of *Tf2*s. WT cells were cultured and collected as in Fig. 1A. The *atg8*$^+$ gene was tagged with CFP and chromosomally integrated for expression from the native promoter. Processing of CFP-tagged Atg8 can serve as a marker for autophagy. During autophagy, free CFP derived from CFP-Atg8 can be detected as shown. (B) *Tf2* mRNAs accumulate in the autophagy mutants *Δatg1* and *Δatg13*. Cells were treated and analyzed as in Fig. 1D. (C) GFP-Tf2 Gag is transported to the vacuole. Each strain expressing GFP-Tf2 Gag was cultured and collected as in Fig. 1A and examined by using fluorescence microscopy. Cpy1–mCherry serves as a vacuole lumen marker. (D) GFP-Tf2 Gag is degraded by autophagy. Each strain expressing GFP-Tf2 Gag was cultured and collected as in Fig. 1A. The ratio of free GFP intensity to GFP-Tf2 Gag intensity was calculated using NIH ImageJ and shown in arbitrary units. Representative experiments are shown (*n*=3).

Journal of Cell Science (2018) 131, jcs221457. doi:10.1242/jcs.221457

both in the WT and *Δtsc2* strains. Although the level at 2 h after nitrogen starvation recovered in the *Δtsc2* strain, the difference of the levels between the WT and *Δtsc2* strains, which was relatively small, might not be biologically significant. We therefore examined Pka1, a kinase regulated by cAMP. Previous studies reported that Pka1 undergoes inhibitory phosphorylation when cells were starved for glucose for several hours or more (Gupta et al., 2011; McInnis et al., 2010). As shown in Fig. S2B (left panel), Pka1 was phosphorylated in WT and *Δtsc2* strains that were first starved for glucose for 6 h and additionally both for glucose and nitrogen for 2 h. The result indicated that Pka1 normally undergoes inhibitory phosphorylation in the *Δtsc2* strain. When cells were simply starved for nitrogen alone for 2 h, *Tf2*s were highly expressed in the *Δtsc2* strain, but Pka1 was not phosphorylated (Fig. S2B, right panel), indicating that Pka1 is not negatively regulated in response to nitrogen starvation.

Taken together, we speculate that a culprit for abnormal induction of *Tf2*s in *Δtsc2* might be a component functioning at the downstream of Pka1 (see Discussion).

Tf2 VLPs degradation by autophagy

Although the results described above show that glucose/cAMP signaling is involved in the regulation of expression of *Tf2*s, it was still unclear how activated Tor2 ($Tor2^{s65}$, Fig. 1D) allowed induction of *Tf2*s upon nitrogen starvation, as was the case in *Δtsc2* cells.

In budding yeast, selective autophagy downregulates transposition of the retrotransposon *Ty1* by eliminating Ty1 virus-like particles (VLPs) from the cytoplasm under nutrient-poor conditions (Suzuki et al., 2011). In addition, autophagy is regulated by Tor2 in many organisms (Blommaart et al., 1995; Noda and Ohsumi, 1998). We thus attempted to examine whether autophagy represses *Tf2*s in fission yeast.

As shown in Figs 1A and 3A, *Tf2*s were slightly induced in WT. In order to reveal the correlation between the onset of autophagy and accumulation of *Tf2*s, we monitored these two events after nitrogen starvation. Expression of *Tf2*s was quickly induced and reached a peak 2 h later in WT (Fig. 4A). We used the marker protein CFP–Atg8 to monitor autophagy. When autophagy is induced, CFP is cut from Atg8, and we can monitor autophagy by detecting free CFP (Sun et al., 2013). After nitrogen starvation, free CFP was detected 2 h later and it kept increasing thereafter (Fig. 4A), suggesting that autophagy, which appeared to be activated at or around the onset of reduction of *Tf2*s, might be responsible for eliminating *Tf2*s in WT. As shown in Fig. 4B, deletion of a gene required for autophagy ($atg1^+$ or $atg13^+$), indeed significantly promoted expression of *Tf2*s.

In budding yeast under nutrient-poor conditions, GFP–Ty1 Gag (Ty1 Gag protein tagged with GFP), which is a component of VLPs, is transported to the vacuolar lumen, where GFP alone is released from GFP-Ty1 Gag by autophagotic proteolysis (Suzuki et al., 2011). As GFP is resistant to further degradation, its fluorescence can be detected in the vacuolar lumen. The activity of autophagy, thus, can be measured with two indices; the amount of free GFP as determined by immunoblotting and the as visualized by assessing internalization of GFP in the vacuolar lumen by a fluorescent microscope. We employed a similar strategy and attempted to test whether *Tf2*s mRNAs were degraded via autophagy in fission yeast.

As shown in Fig. 4C, fission yeast GFP–Tf2 Gag was localized as distinct dots in cytoplasm 2 h after nitrogen starvation. In cells lacking $atg1^+$, a gene essential for initiation of autophagy, GFP–Tf2 Gag remained around the vacuole, but was not transported to the vacuolar lumen 12 h after nitrogen starvation (Fig. 4C). We also found that during autophagy, free GFP derived from GFP–Tf2 Gag was detected in WT cells, but not in *Δatg1* cells (Fig. 4D). Taken together, these results suggest that fission yeast GFP–Tf2 Gag is not degraded by autophagy.

Inactivation of Tor2 causes autophagy and represses expression of *Tf2*s

Having shown that expression of fission yeast *Tf2*s is repressed by autophagy, we next attempted to investigate a role of Tor2, a key regulator of autophagy, in the regulation of *Tf2*s. Under nutrient-rich conditions, Tor2 is activated and inhibits autophagy. In $tor2^{ts10}$ mutant cells, Tor2 is inactivated at the restrictive temperature regardless of nitrogen availability (Matsuo et al., 2007), and allows the onset of autophagy.

Apb1 is a fission yeast homolog of human CENP-B, and inhibits expression of *Tf2*s. In the *Δabp1* mutant, *Tf2*s are constitutively expressed even under nitrogen-rich conditions (Cam et al., 2008). Inactivation of Tor2 in *Δabp1* thus allowed us to assess the contribution of autophagy to the elimination of *Tf2* mRNAs under nitrogen-rich conditions. As CFP–Atg8 is processed by proteolysis and CFP is released upon the onset of autophagy (Mukaiyama et al., 2009; Sun et al., 2013), it was used as an indicator of the activity of autophagy. As shown in Fig. 5A, upon the shift to a restrictive temperature of $tor2^{ts10}$ (30°C), CFP was released from CFP–Atg8 and expression of *Tf2*s was gradually decreased in the *Δabp1*

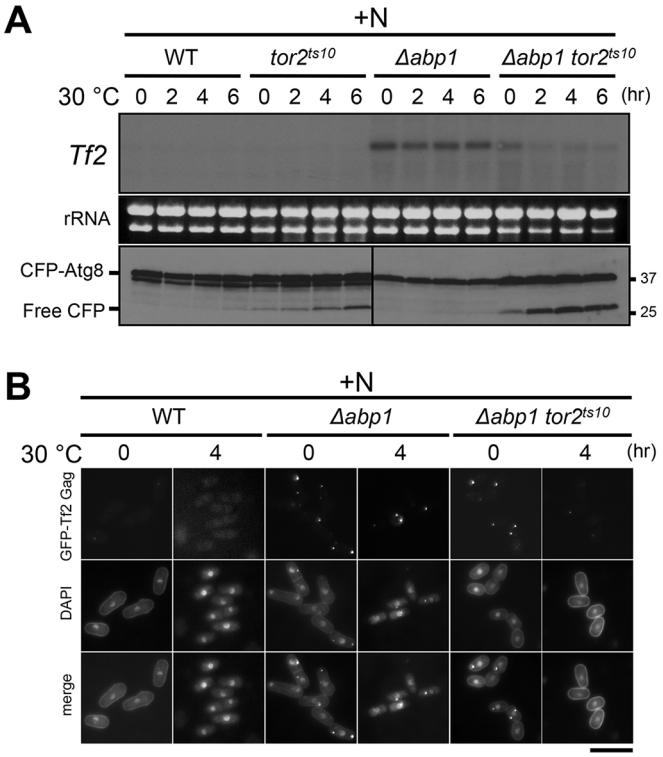

Fig. 5. Role of mTOR in repression of autophagy. (A) Under nitrogen-rich conditions, the $tor2^{ts10}$ mutant induces autophagy and suppresses expression of *Tf2*s in *Δabp1* cells. At the restrictive temperature (30°C), $tor2^{ts10}$ could cause autophagy even in nitrogen-rich conditions. *Tf2*s were constitutively expressed in the *Δabp1* mutant. Each strain expressed CFP–Atg8 and was grown to mid-log phase at 26°C and then shifted to 30°C for the indicated time. (B) GFP-Tf2 Gag signals disappeared in $tor2^{ts10}$ *Δabp1* cells grown at 30°C for 4 h. Cells were cultured and collected as in A and examined by using fluorescence microscopy. Scale bar: 10 µm.

Journal of Cell Science (2018) 131, jcs221457. doi:10.1242/jcs.221457

tor2^{ts10} double mutant. Furthermore, we observed the localization of GFP-Tf2 Gag and found that GFP-Tf2 Gag, which was able to form VLPs in the cytoplasm in *Δabp1 tor2*^{ts10} at the permissive temperature (26°C), almost disappeared after the shift to 30°C for 4 h (Fig. 5B). These results suggest that autophagy can be a primary means to repress expression of *Tf2*s, and Tor2 activity had a great influence on it.

Induction of *Tf2*s due to suppression of autophagy in *Δtsc2* cells

As a loss of Tsc2 resulted in activation of Tor2 even under nitrogen-poor conditions (Matsuo et al., 2007), we hypothesized that the strong induction of *Tf2*s in *Δtsc2* cells under nitrogen starvation was, at least in part, attributable to suppression of autophagy by Tor2. Supporting this hypothesis, the activity of autophagy, as measured by release of CFP from CFP–Atg8, is lower in *Δtsc2* cells than that in WT (Fig. 6A). We also found that *Tf2*s were significantly expressed in *Δatg1* upon nitrogen starvation, but that *Δatg1* did not have any additive contribution to the level of *Tf2*s in *Δtsc2 Δatg1* cells (Fig. 6B). In addition, we found that *tor2*^{ts10}, when introduced into *Δtsc2* cells, could allow the onset of autophagy, which, in turn, suppresses *Tf2*s expression (Fig. 6C,D). It should be noted that the level of *Tf2*s induced in *tor2*^{ts10} was lower than that in WT (Fig. 6D), suggesting that Tor2 might play a role in promoting expression of *Tf2*s under nitrogen-poor conditions.

Taken together, these results prove our hypothesis that the high level of expression of *Tf2*s in *Δtsc2* cells was due to Tor2 activation, even under nitrogen starvation, which suppressed autophagy.

Functional relationship between autophagy and glucose/cAMP signaling

Finally, we investigated the relationship between autophagy and the glucose/cAMP signaling, which was shown to regulate expression of *Tf2*s (Figs 2 and 3). We found that *Δpka1* almost completely suppressed expression of *Tf2*s in *Δatg1* after nitrogen starvation (Fig. 7A), indicating that Pka1 was required for induction of *Tf2*s even when autophagy was suppressed. Furthermore, the level of *Tf2*s in *Δcgs2 Δatg1* double mutant were higher than each of the single mutants (Fig. 7B). These results suggested that the glucose/cAMP signaling and autophagy regulated expression of *Tf2*s in parallel.

DISCUSSION

We have shown here that *Tf2*s are abnormally induced in*Δtsc2*, *rhb1-DA4* and *tor2*^{s65} cells, all of which activate the RHEB–mTOR axis even under nitrogen-poor conditions. The results of the subsequent study suggested that abnormal induction of *Tf2*s is due to a failure in, at least, two processes: downregulation of the glucose/cAMP signaling pathway and RHEB–mTOR axis, and induction of autophagy that normally degrades *Tf2* mRNAs.

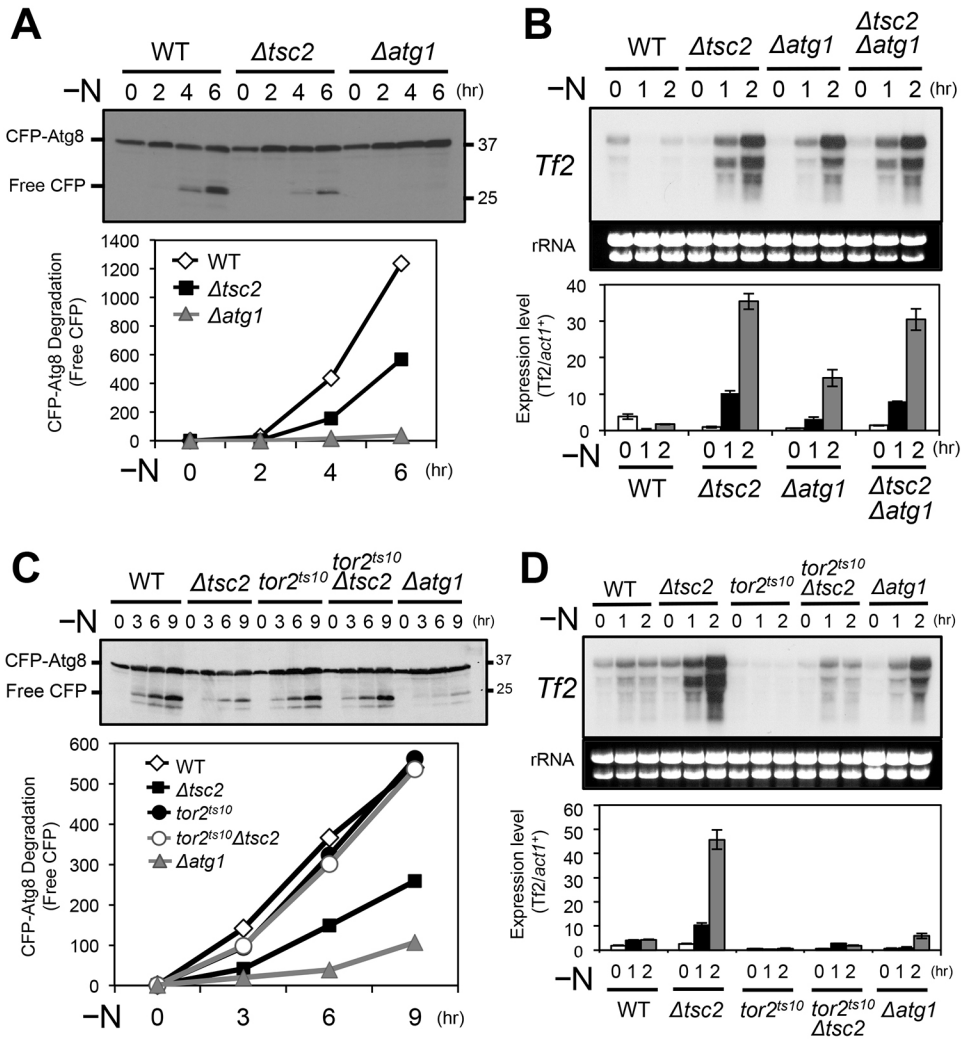

Fig. 6. Induction of *Tf2*s due to suppression of autophagy in *Δtsc2* cells. (A) There is a low level of autophagy induced in *Δtsc2* cells after nitrogen starvation (–N). Each strain expressing CFP–Atg8 was cultured as treated and analyzed as in Fig. 4A. The top panel shows western blot analysis. The lower panel shows the quantification of the result shown in the top panel. The free CFP intensity was calculated using NIH ImageJ and shown in arbitrary units. (B) The *Δtsc2* mutant expresses more *Tf2*s than the autophagy mutant *Δatg1*. Cells were treated and analyzed as in Fig. 1C. The top panel shows northern blot analysis. The lower panel shows the qRT-PCR of *Tf2* mRNA levels. (C) *tor2*^{ts10} suppresses the autophagy defect in *Δtsc2* cells. Each strain expressing CFP–Atg8 was treated and analyzed as in Fig. 4A. The top panel shows western analysis. The lower panel shows the quantification of the result shown in the top panel. The free CFP intensity was calculated using NIH ImageJ and shown in arbitrary units. (D) *tor2*^{ts10} suppresses *Tf2*s expression in *Δtsc2*. Each strain was analyzed as in Fig. 2E. The top panel shows northern blot analysis. The lower panel shows the qRT-PCR of *Tf2* mRNA levels. Results shown in A and C are a representative experiment (n=3). In B and D, the data are presented as mean±s.e.m. (n=3).

Journal of Cell Science (2018) 131, jcs221457. doi:10.1242/jcs.221457

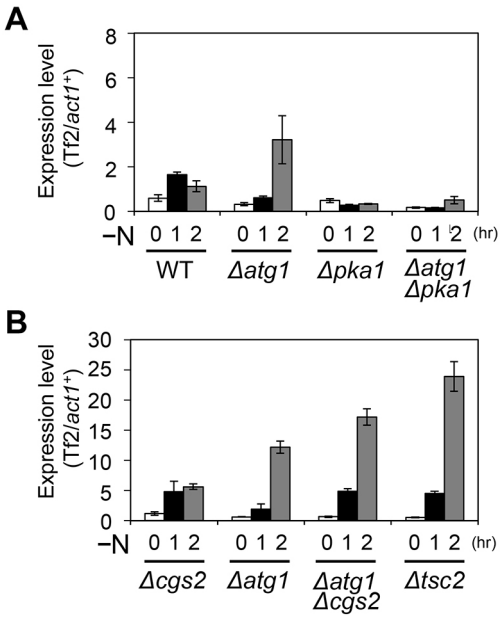

Fig. 7. The glucose/cAMP signaling pathway functions in parallel to autophagy. (A) *Δpka1* suppresses expression of *Tf2*s in *Δatg1*. Cells were treated and analyzed as in Fig. 1C. (B) Expression of *Tf2*s in the *Δatg1 Δcgs2* double mutant is higher than in each single mutant. Cells were treated and analyzed as in Fig. 1C. The data are presented as mean±s.e.m. (*n*=3).

Regulation of the glucose/cAMP signaling pathway by RHEB–mTOR axis

Our screen for multicopy suppressors of *Δtsc2* identified the *cgs2*$^+$ gene, a negative regulator of the glucose/cAMP signaling pathway. In addition to overexpression of the *cgs2*$^+$ gene, deletion of *cyr1*$^+$, *pka1*$^+$ and *tor1*$^+$, all of which are required for the glucose/cAMP signaling pathway, can suppress abnormal induction of *Tf2*s in *Δtsc2* upon nitrogen starvation. Likewise, abnormal induction of *Tf2*s in cells with a dominant-active mutant of the Rhb1 GTPase (*rhb1-DA4*) can be suppressed by overexpression of the *cgs2*$^+$ gene as well as deletion of *pka1*$^+$. These results indicate that induction of *Tf2*s in *Δtsc2* and *rhb1-DA4* cells is, at least in part, attributable to abnormal activation of the glucose/cAMP signaling pathway. We propose that, although the activity of the glucose/cAMP signaling pathway is directly regulated by the availability of glucose, it is also regulated by the RHEB–mTOR axis depending on the availability of nitrogen (Fig. 8). This way, cellular proliferation/metabolism can be controlled in a manner that is coordinated with the availability of both glucose and nitrogen. In *Δtsc2* and *rhb1-DA4* mutants, the RHEB–mTOR axis continuously stimulates the glucose/cAMP signaling pathway even when cells are starved for nitrogen. Our biochemical analysis (the level of cAMP and inhibitory phosphorylation of Pka1) indicated that Pka1 is normally regulated in *Δtsc2*. We thus speculate that the RHEB–mTOR axis targets a component of the glucose/cAMP signaling pathway that is downstream of Pka1. Although a number of proteins have been identified as targets of mTOR kinase (Otsubo et al., 2017), none of them are involved in the glucose/cAMP signaling pathway. Future study is needed to understand how the RHEB–mTOR axis regulates the glucose/cAMP signaling pathway.

Degradation of *Tf2*s by autophagy

Because deletion of *cyr1*$^+$ and *pka1*$^+$ in *Δtsc2* cells still allows expression of *Tf2*s at a level higher than in WT cells upon nitrogen starvation, we suspected that another mechanism was involved in the regulation of *Tf2*s. Guided by a previous study in budding yeast (Suzuki et al., 2011), we have tested here whether autophagy is responsible for degradation of *Tf2* mRNAs. Our analysis has shown that: (1) the autophagic activity increases upon nitrogen starvation, and (2) even under nitrogen-rich conditions, autophagic activity also increases when Tor2 is inactivated. We have also confirmed that deletion of a gene required for autophagy (*atg1*$^+$ or *atg13*$^+$) allows accumulation of *Tf2* mRNAs upon nitrogen starvation. These results indicate that continuous activation of RHEB–mTOR axis in *Δtsc2* and *rhb1-DA4* mutants prevents induction of autophagy targeting *Tf2* mRNAs (Fig. 8).

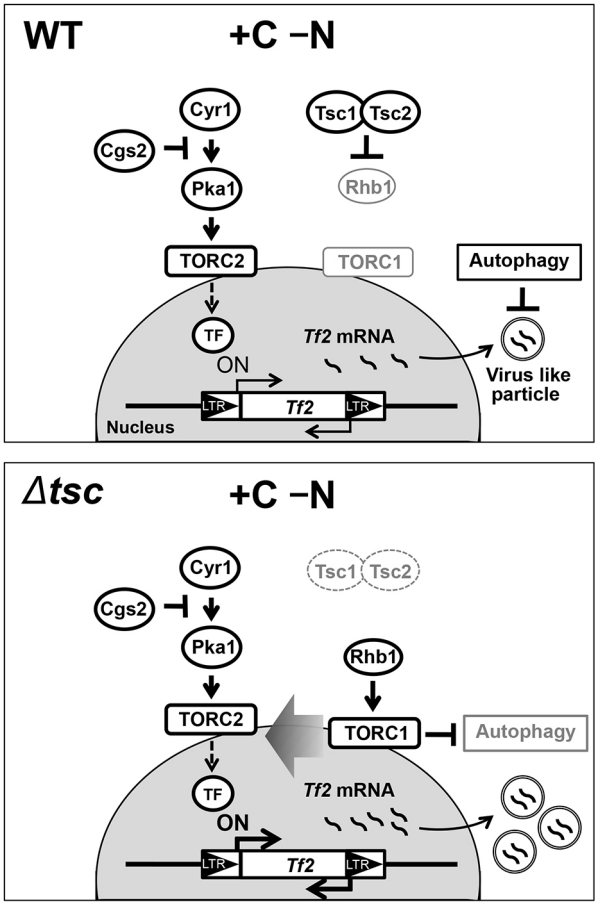

Fig. 8. A model for the regulation of expression of *Tf2*s under nitrogen starvation. In WT cells upon nitrogen starvation (–N), the RHEB–mTOR axis, which is inactivated by Tsc2, no longer activates the glucose/cAMP signaling pathway, which promotes expression of *Tf2*s via Atf1 and/or another transcriptional factor (TF). Inactivation of RHEB–mTOR axis also allows induction of autophagy targeting *Tf2 mRNA*s. In *Δtsc1/2* cells, the RHEB–mTOR axis, which is active even under nitrogen-poor conditions, continuously induces expression of *Tf2*s and inhibits autophagy, causing accumulation of *Tf2* mRNAs.

Although RHEB–mTOR axis is continuously activated in *Δtsc2* and *rhb1-DA4* mutants, *Tf2*s are not abnormally induced under nitrogen-rich conditions. Nitrogen starvation is therefore a crucial requirement for induction of *Tf2*s. Expression of *Tf2*s is silenced by multiple mechanisms, including chromatin-mediated mechanisms, such as binding of CENP-B homologs (Cam et al., 2008; Lorenz et al., 2014), histone modifications (Lorenz et al., 2014) and histone chaperones (Anderson et al., 2009), as well as by RNA-mediated mechanisms (Woolcock et al., 2011; Yamanaka et al., 2013). We speculate that silencing by some of these mechanisms is relieved upon nitrogen starvation.

Previous works have demonstrated that some of the fission yeast retrotransposons induced in response to various forms of stress are integrated into the promoters of the stress-responsive genes, suggesting a role of induction of retrotransposons in adaptation (Feng et al., 2013; Sehgal et al., 2007). In this study, we have shown that *Tf2*s in the WT cells are transiently induced in response to nitrogen starvation. Some of these *Tf2*s may contribute to adaptation. We have also shown that expression/accumulation of *Tf2*s induced in the WT cells are effectively suppressed by the RHEB–mTOR axis, likely for protection of the genome integrity. Human endogenous retroviruses (HERVs), which occupy ∼8% of the human genome, have been shown to be a cause of neurological disorders (Küry et al., 2018). Because our study with fission yeast has shown that retrotransposons are abnormally induced in *Δtsc2* cells, loss of the *TSC2* gene in humans may allow abnormal expression of HERVs, which may, in turn, contribute to the symptoms of the disease TSC, as well as other neurological disorders.

MATERIALS AND METHODS

Yeast strains and growth media

The *S. pombe* strains used in this study are listed in Table S1. *S. pombe* cells were grown in YEA and EMM containing the appropriate nutrient supplements as described previously (Moreno et al., 1991). The incubation temperature was 26°C. All yeast transformations were performed with the lithium acetate method (Gietz et al., 1992; Okazaki et al., 1990).

Screen for multicopy suppressors of *Δtsc2*

The *Δtsc2* mutants (AE512) were transformed with an *S. pombe* genomic library containing the partially digested *Sau3A*I DNA fragment constructed in a multicopy plasmid, pAL-KS (Tanaka et al., 2001). Plasmids were recovered from canavanine-resistant and Leu^+ transformants, and their nucleotide sequences were determined. A BLAST search was performed to identify the obtained sequences, and the region covered by the inserted genomic sequence was determined.

Northern blot analysis

Total RNA was prepared from cultured *S. pombe* as described previously (Jensen et al., 1983) and fractionated on a 0.8% gel containing 3.7% formaldehyde (Thomas, 1980). The probe for *Tf2* was PCR-amplified from a *S. pombe* genomic DNA library and labeled with [α-^{32}P]dCTP using standard methods. The *Tf2* primer sets used were: 5′-ATGTCCTACGCA-AATTATCGTTATATG-3′, 5′-CTTGTACTTTCCCTGTTTGTCTG-3′. This probe contained the conserved *Tf2* element sequence.

qRT-PCR

Total RNAs were prepared from cultured *S. pombe* as described previously (Jensen et al., 1983). Aliquots of total RNA were used for the synthesis of cDNA by the ReverTra Ace quantitative real-time RT-PCR (qRT-PCR) Master Mix with gDNA Remover (TOYOBO) in accordance with the manufacturer's instructions. The synthesized cDNAs were quantified using MyiQ2 (Bio-Rad) and SYBR qPCR Mix (Bio-Rad). Expression profiles for individual *Tf2* cDNAs were normalized against *act1*$^+$ cDNA levels. The primer sets used were: for Tf2-13, 5′-CTGGAAATGGACACCAACA-CAA-3′, 5′-TACGGCTCCTACAGCGACATCT-3′; for act1$^+$, 5′-CTTTCT-ACAACGAGCTTCGTGTTG-3′, 5′-GAGTCATCTTCTCACGGTTGGAT-3′. Data are presented as mean±s.e.m.

Microscopy

Cells were observed with an Axioplan2 imaging digital microscope (ZEISS) and a AxioCam MRm digital CCD camera (ZEISS).

CFP–Atg8 processing assay

Cell lysates were prepared using a post-alkaline extraction method (Matsuo et al., 2006) and a boiling-SDS-glass bead method (Masai et al., 1995). Samples were separated by 4–20% SDS-PAGE (Bio-Rad) and immunoblotted with an anti-GFP antibody [1:1000, #11814460001, Roche, clones 7.1 and 13.1 (Prasher et al., 1992)].

Western blotting

Cell lysates were prepared using a Laemmli buffer method (Masai et al., 1995). Samples were separated by 4–20% SDS-PAGE (Bio-Rad) and immunoblotted with an anti-GFP antibody [1:1000, #11814460001, Roche, clones 7.1 and 13.1 (Prasher et al., 1992)]. Blots were also probed with the anti-α-tubulin antibody TAT-1 (1:10,000, gift from Keith Gull, University of Manchester, UK), to normalize protein loading. Immunoreactive bands were visualized by chemiluminescence (Thermo) with horseradish peroxidase-conjugated sheep anti-mouse IgG (GE Healthcare) antibody.

cAMP assay

The level of cAMP was measured using a commercial kit (GE Healthcare). At intervals, aliquots were taken, mixed with an equal volume of 10% trichloroacetic acid (TCA) and frozen in liquid nitrogen for 10 min. After thawing, samples were kept at 4°C overnight. Cell debris was removed by centrifugation (13,400 ***g*** for 5 min), and the supernatants were repeatedly extracted with water-saturated ether to remove TCA. The cAMP content was determined according to the supplier's instructions.

Acknowledgements

We thank Yuko Takayama (Teikyo University, Japan) for GFP-Tf2 strains and useful discussion, Du LL (National Institute of Biological Sciences at Beijing, China) for the autophagy strains, Kaoru Takegawa (Kyushu University, Japan) for the autophagy plasmids, strains and useful discussion, Keith Gull (University of Manchester, UK) for the anti-α-tubulin antibody (TAT-1), Masayuki Yamamoto (National Institute for Basic Biology, Japan) for the *tor2* mutant strains and the Yeast Genetic Resource Center of Japan, supported by the National BioResource Project (NBRP/YGRC), for the *S. pombe* strains, plasmids and genomic library. We also thank members of the Matsumoto laboratory for helpful discussion.

Competing interests

The authors declare no competing or financial interests.

Author contributions

Conceptualization: Y.N., T.M.; Methodology: Y.N., T.M.; Software: Y.N.; Validation: Y.N.; Formal analysis: Y.N.; Investigation: Y.N.; Resources: Y.N.; Data curation: Y.N., T.M.; Writing - original draft: Y.N.; Writing - review & editing: Y.N., T.M.; Visualization: Y.N.; Supervision: T.M.; Project administration: T.M.; Funding acquisition: Y.N., T.M.

Funding

This study was supported by Japan Society for the Promotion of Science (JSPS) KAKENHI grant numbers JP19657039, JP12J40002 (to Y.N.) and a Sasakawa Grant for Science Fellows (SGSF) from the Japan Science Society (to Y.N.).

Supplementary information

Supplementary information available online at
http://jcs.biologists.org/lookup/doi/10.1242/jcs.221457.supplemental

References

Anderson, H. E., Wardle, J., Korkut, S. V., Murton, H. E., Lopez-Maury, L., Bahler, J. and Whitehall, S. K. (2009). The fission yeast HIRA histone chaperone is required for promoter silencing and the suppression of cryptic antisense transcripts. *Mol. Cell. Biol.* **29**, 5158-5167.

Baillie, J. K., Barnett, M. W., Upton, K. R., Gerhardt, D. J., Richmond, T. A., De Sapio, F., Brennan, P. M., Rizzu, P., Smith, S., Fell, M. et al. (2011). Somatic retrotransposition alters the genetic landscape of the human brain. *Nature* **479**, 534-537.

Blommaart, E. F. C., Luiken, J. J. F. P., Blommaart, P. J. E., van Woerkom, G. M. and Meijer, A. J. (1995). Phosphorylation of ribosomal protein S6 is inhibitory for autophagy in isolated rat hepatocytes. *J. Biol. Chem.* **270**, 2320-2326.

Cam, H. P., Noma, K.-I., Ebina, H., Levin, H. L. and Grewal, S. I. S. (2008). Host genome surveillance for retrotransposons by transposon-derived proteins. *Nature* **451**, 431-436.

Capy, P., Gasperi, G., Biémont, C. and Bazin, C. (2000). Stress and transposable elements: co-evolution or useful parasites? *Heredity* **85**, 101-106.

Cohen, A., Kupiec, M. and Weisman, R. (2014). Glucose activates TORC2-Gad8 protein via positive regulation of the cAMP/cAMP-dependent protein kinase A

(PKA) pathway and negative regulation of the Pmk1 protein-mitogen-activated protein kinase pathway. *J. Biol. Chem.* **289**, 21727-21737.
Crichton, J. H., Dunican, D. S., Maclennan, M., Meehan, R. R. and Adams, I. R. (2014). Defending the genome from the enemy within: mechanisms of retrotransposon suppression in the mouse germline. *Cell. Mol. Life Sci.* **71**, 1581-1605.
Dumesic, P. A. and Madhani, H. D. (2014). Recognizing the enemy within: licensing RNA-guided genome defense. *Trends Biochem. Sci.* **39**, 25-34.
European Chromosome 16 Tuberous Sclerosis Consortium. (1993). Identification and characterization of the tuberous sclerosis gene on chromosome 16. *Cell* **75**, 1305-1315.
Evsikov, A. V., Graber, J. H., Brockman, J. M., Hampl, A., Holbrook, A. E., Singh, P., Eppig, J. J., Solter, D. and Knowles, B. B. (2006). Cracking the egg: molecular dynamics and evolutionary aspects of the transition from the fully grown oocyte to embryo. *Genes Dev.* **20**, 2713-2727.
Feng, G., Leem, Y.-E. and Levin, H. L. (2013). Transposon integration enhances expression of stress response genes. *Nucleic Acids Res.* **41**, 775-789.
Fingar, D. C. and Blenis, J. (2004). Target of rapamycin (TOR): an integrator of nutrient and growth factor signals and coordinator of cell growth and cell cycle progression. *Oncogene* **23**, 3151-3171.
Garami, A., Zwartkruis, F. J. T., Nobukuni, T., Joaquin, M., Roccio, M., Stocker, H., Kozma, S. C., Hafen, E., Bos, J. L. and Thomas, G. (2003). Insulin activation of Rheb, a mediator of mTOR/S6K/4E-BP signaling, is inhibited by TSC1 and 2. *Mol. Cell* **11**, 1457-1466.
Gietz, D., St Jean, A., Woods, R. A. and Schiestl, R. H. (1992). Improved method for high efficiency transformation of intact yeast cells. *Nucleic Acids Res.* **20**, 1425.
Gupta, D. R., Paul, S. K., Oowatari, Y., Matsuo, Y. and Kawamukai, M. (2011). Complex formation, phosphorylation, and localization of protein kinase A of Schizosaccharomyces pombe upon glucose starvation. *Biosci. Biotechnol. Biochem.* **75**, 1456-1465.
Hoff, E. F., Levin, H. L. and Boeke, J. D. (1998). Schizosaccharomyces pombe retrotransposon Tf2 mobilizes primarily through homologous cDNA recombination. *Mol. Cell. Biol.* **18**, 6839-6852.
Hutnick, L. K., Huang, X., Loo, T.-C., Ma, Z. and Fan, G. (2010). Repression of retrotransposal elements in mouse embryonic stem cells is primarily mediated by a DNA methylation-independent mechanism. *J. Biol. Chem.* **285**, 21082-21091.
Inoki, K., Li, Y., Zhu, T., Wu, J. and Guan, K.-L. (2002). TSC2 is phosphorylated and inhibited by Akt and suppresses mTOR signalling. *Nat. Cell Biol.* **4**, 648-657.
Jensen, R., Sprague, G. F., Jr. and Herskowitz, I. (1983). Regulation of yeast mating-type interconversion: feedback control of HO gene expression by the mating-type locus. *Proc. Natl. Acad. Sci. USA* **80**, 3035-3039.
Kanoh, J., Watanabe, Y., Ohsugi, M., Iino, Y. and Yamamoto, M. (1996). Schizosaccharomyces pombe gad7+ encodes a phosphoprotein with a bZIP domain, which is required for proper G1 arrest and gene expression under nitrogen starvation. *Genes Cells* **1**, 391-408.
Kawai, M., Nakashima, A., Ueno, M., Ushimaru, T., Aiba, K., Doi, H. and Uritani, M. (2001). Fission yeast tor1 functions in response to various stresses including nitrogen starvation, high osmolarity, and high temperature. *Curr. Genet.* **39**, 166-174.
Küry, P., Nath, A., Créange, A., Dolei, A., Marche, P., Gold, J., Giovannoni, G., Hartung, H.-P. and Perron, H. (2018). Human endogenous retroviruses in neurological diseases. *Trends Mol. Med.* **24**, 379-394.
Kwiatkowski, D. J. and Short, M. P. (1994). Tuberous sclerosis. *Arch. Dermatol.* **130**, 348-354.
Leung, D. C. and Lorincz, M. C. (2012). Silencing of endogenous retroviruses: when and why do histone marks predominate? *Trends Biochem. Sci.* **37**, 127-133.
Li, Z., Dai, H., Martos, S. N., Xu, B., Gao, Y., Li, T., Zhu, G., Schones, D. E. and Wang, Z. (2015). Distinct roles of DNMT1-dependent and DNMT1-independent methylation patterns in the genome of mouse embryonic stem cells. *Genome Biol.* **16**, 115.
Lorenz, D. R., Meyer, L. F., Grady, P. J. R., Meyer, M. M. and Cam, H. P. (2014). Heterochromatin assembly and transcriptome repression by Set1 in coordination with a class II histone deacetylase. *eLife* **3**, e04506.
Macfarlan, T. S., Gifford, W. D., Driscoll, S., Lettieri, K., Rowe, H. M., Bonanomi, D., Firth, A., Singer, O., Trono, D. and Pfaff, S. L. (2012). Embryonic stem cell potency fluctuates with endogenous retrovirus activity. *Nature* **487**, 57-63.
Mach, K. E., Furge, K. A. and Albright, C. F. (2000). Loss of Rhb1, a Rheb-related GTPase in fission yeast, causes growth arrest with a terminal phenotype similar to that caused by nitrogen starvation. *Genetics* **155**, 611-622.
Manning, B. D. and Cantley, L. C. (2003). Rheb fills a GAP between TSC and TOR. *Trends Biochem. Sci.* **28**, 573-576.
Masai, H., Miyake, T. and Arai, K. (1995). hsk1+, a Schizosaccharomyces pombe gene related to Saccharomyces cerevisiae CDC7, is required for chromosomal replication. *EMBO J.* **14**, 3094-3104.
Mata, J., Wilbrey, A. and Bähler, J. (2007). Transcriptional regulatory network for sexual differentiation in fission yeast. *Genome Biol.* **8**, R217.
Matsumoto, S., Bandyopadhyay, A., Kwiatkowski, D. J., Maitra, U. and Matsumoto, T. (2002). Role of the Tsc1-Tsc2 complex in signaling and transport across the cell membrane in the fission yeast Schizosaccharomyces pombe. *Genetics* **161**, 1053-1063.
Matsuo, Y., Asakawa, K., Toda, T. and Katayama, S. (2006). A rapid method for protein extraction from fission yeast. *Biosci. Biotechnol. Biochem.* **70**, 1992-1994.
Matsuo, T., Otsubo, Y., Urano, J., Tamanoi, F. and Yamamoto, M. (2007). Loss of the TOR kinase Tor2 mimics nitrogen starvation and activates the sexual development pathway in fission yeast. *Mol. Cell. Biol.* **27**, 3154-3164.
Matviw, H., Li, J. H. and Young, D. (1993). The Schizosaccharomyces pombe pde1/cgs2 gene encodes a cyclic AMP phosphodiesterase. *Biochem. Biophys. Res. Commun.* **194**, 79-82.
McClintock, B. (1950). The origin and behavior of mutable loci in maize. *Proc. Natl. Acad. Sci. USA* **36**, 344-355.
McInnis, B., Mitchell, J. and Marcus, S. (2010). Phosphorylation of the protein kinase A catalytic subunit is induced by cyclic AMP deficiency and physiological stresses in the fission yeast, Schizosaccharomyces pombe. *Biochem. Biophys. Res. Commun.* **399**, 665-669.
Moreno, S., Klar, A. and Nurse, P. (1991). Molecular genetic analysis of fission yeast Schizosaccharomyces pombe. *Methods Enzymol.* **194**, 795-823.
Mukaiyama, H., Kajiwara, S., Hosomi, A., Giga-Hama, Y., Tanaka, N., Nakamura, T. and Takegawa, K. (2009). Autophagy-deficient Schizosaccharomyces pombe mutants undergo partial sporulation during nitrogen starvation. *Microbiology* **155**, 3816-3826.
Muotri, A. R., Chu, V. T., Marchetto, M. C. N., Deng, W., Moran, J. V. and Gage, F. H. (2005). Somatic mosaicism in neuronal precursor cells mediated by L1 retrotransposition. *Nature* **435**, 903-910.
Murai, T., Nakase, Y., Fukuda, K., Chikashige, Y., Tsutsumi, C., Hiraoka, Y. and Matsumoto, T. (2009). Distinctive responses to nitrogen starvation in the dominant active mutants of the fission yeast Rheb GTPase. *Genetics* **183**, 517-527.
Nakase, Y., Fukuda, K., Chikashige, Y., Tsutsumi, C., Morita, D., Kawamoto, S., Ohnuki, M., Hiraoka, Y. and Matsumoto, T. (2006). A defect in protein farnesylation suppresses a loss of Schizosaccharomyces pombe tsc2+, a homolog of the human gene predisposing to tuberous sclerosis complex. *Genetics* **173**, 569-578.
Nakase, Y., Nakase, M., Kashiwazaki, J., Murai, T., Otsubo, Y., Mabuchi, I., Yamamoto, M., Takegawa, K. and Matsumoto, T. (2013). The fission yeast beta-arrestin-like protein Any1 is involved in TSC-Rheb signaling and the regulation of amino acid transporters. *J. Cell Sci.* **126**, 3972-3981.
Noda, T. and Ohsumi, Y. (1998). Tor, a phosphatidylinositol kinase homologue, controls autophagy in yeast. *J. Biol. Chem.* **273**, 3963-3966.
Okazaki, K., Okazaki, N., Kume, K., Jinno, S., Tanaka, K. and Okayama, H. (1990). High-frequency transformation method and library transducing vectors for cloning mammalian cDNAs by trans-complementation of Schizosaccharomyces pombe. *Nucleic Acids Res.* **18**, 6485-6489.
Otsubo, Y., Nakashima, A., Yamamoto, M. and Yamashita, A. (2017). TORC1-Dependent Phosphorylation Targets in Fission Yeast. *Biomolecules* **7**, 50.
Peaston, A. E., Evsikov, A. V., Graber, J. H., de Vries, W. N., Holbrook, A. E., Solter, D. and Knowles, B. B. (2004). Retrotransposons regulate host genes in mouse oocytes and preimplantation embryos. *Dev. Cell* **7**, 597-606.
Prasher, D. C., Eckenrode, V. K., Ward, W. W., Prendergast, F. G. and Cormier, M. J. (1992). Primary structure of the Aequorea victoria green-fluorescent protein. *Gene* **111**, 229-233.
Raught, B., Gingras, A.-C. and Sonenberg, N. (2001). The target of rapamycin (TOR) proteins. *Proc. Natl. Acad. Sci. USA* **98**, 7037-7044.
SanMiguel, P., Tikhonov, A., Jin, Y.-K., Motchoulskaia, N., Zakharov, D., Melake-Berhan, A., Springer, P. S., Edwards, K. J., Lee, M., Avramova, Z. et al. (1996). Nested retrotransposons in the intergenic regions of the maize genome. *Science* **274**, 765-768.
Sehgal, A., Lee, C.-Y. S. and Espenshade, P. J. (2007). SREBP controls oxygen-dependent mobilization of retrotransposons in fission yeast. *PLoS Genet.* **3**, e131.
Stephan, J. S., Yeh, Y.-Y., Ramachandran, V., Deminoff, S. J. and Herman, P. K. (2009). The Tor and PKA signaling pathways independently target the Atg1/Atg13 protein kinase complex to control autophagy. *Proc. Natl. Acad. Sci. USA* **106**, 17049-17054.
Sun, L.-L., Li, M., Suo, F., Liu, X.-M., Shen, E.-Z., Yang, B., Dong, M.-Q., He, W.-Z. and Du, L.-L. (2013). Global analysis of fission yeast mating genes reveals new autophagy factors. *PLoS Genet.* **9**, e1003715.
Suzuki, K., Morimoto, M., Kondo, C. and Ohsumi, Y. (2011). Selective autophagy regulates insertional mutagenesis by the Ty1 retrotransposon in Saccharomyces cerevisiae. *Dev. Cell* **21**, 358-365.
Swanstrom, R. and Wills, J. W. (1997). Synthesis, assembly, and processing of viral proteins. In *Retroviruses*, pp. 263-334. (ed. J. M. Coffin, S. H. Hughes and H. E. Varmus). NY: Cold Spring Harbor.
Tanaka, K., Hao, Z., Kai, M. and Okayama, H. (2001). Establishment and maintenance of sister chromatid cohesion in fission yeast by a unique mechanism. *EMBO J.* **20**, 5779-5790.
Thomas, P. S. (1980). Hybridization of denatured RNA and small DNA fragments transferred to nitrocellulose. *Proc. Natl. Acad. Sci. USA* **77**, 5201-5205.
van Slegtenhorst, M., de Hoogt, R., Hermans, C., Nellist, M., Janssen, B., Verhoef, S., Lindhout, D., van den Ouweland, A., Halley, D., Young, J. et al.

(1997). Identification of the tuberous sclerosis gene TSC1 on chromosome 9q34. *Science* **277**, 805-808.

van Slegtenhorst, M., Carr, E., Stoyanova, R., Kruger, W. D. and Henske, E. P. (2004). Tsc1+ and tsc2+ regulate arginine uptake and metabolism in Schizosaccharomyces pombe. *J. Biol. Chem.* **279**, 12706-12713.

Wang, L., Griffiths, K., Jr, Zhang, Y. H., Ivey, F. D. and Hoffman, C. S. (2005). Schizosaccharomyces pombe adenylate cyclase suppressor mutations suggest a role for cAMP phosphodiesterase regulation in feedback control of glucose/cAMP signaling. *Genetics* **171**, 1523-1533.

Weisman, R. and Choder, M. (2001). The fission yeast TOR homolog, tor1+, is required for the response to starvation and other stresses via a conserved serine. *J. Biol. Chem.* **276**, 7027-7032.

Weisman, R., Roitburg, I., Schonbrun, M., Harari, R. and Kupiec, M. (2007). Opposite effects of tor1 and tor2 on nitrogen starvation responses in fission yeast. *Genetics* **175**, 1153-1162.

Welton, R. M. and Hoffman, C. S. (2000). Glucose monitoring in fission yeast via the Gpa2 galpha, the git5 Gbeta and the git3 putative glucose receptor. *Genetics* **156**, 513-521.

Woolcock, K. J., Gaidatzis, D., Punga, T. and Bühler, M. (2011). Dicer associates with chromatin to repress genome activity in Schizosaccharomyces pombe. *Nat. Struct. Mol. Biol.* **18**, 94-99.

Yamanaka, S., Mehta, S., Reyes-Turcu, F. E., Zhuang, F., Fuchs, R. T., Rong, Y., Robb, G. B. and Grewal, S. I. S. (2013). RNAi triggered by specialized machinery silences developmental genes and retrotransposons. *Nature* **493**, 557-560.

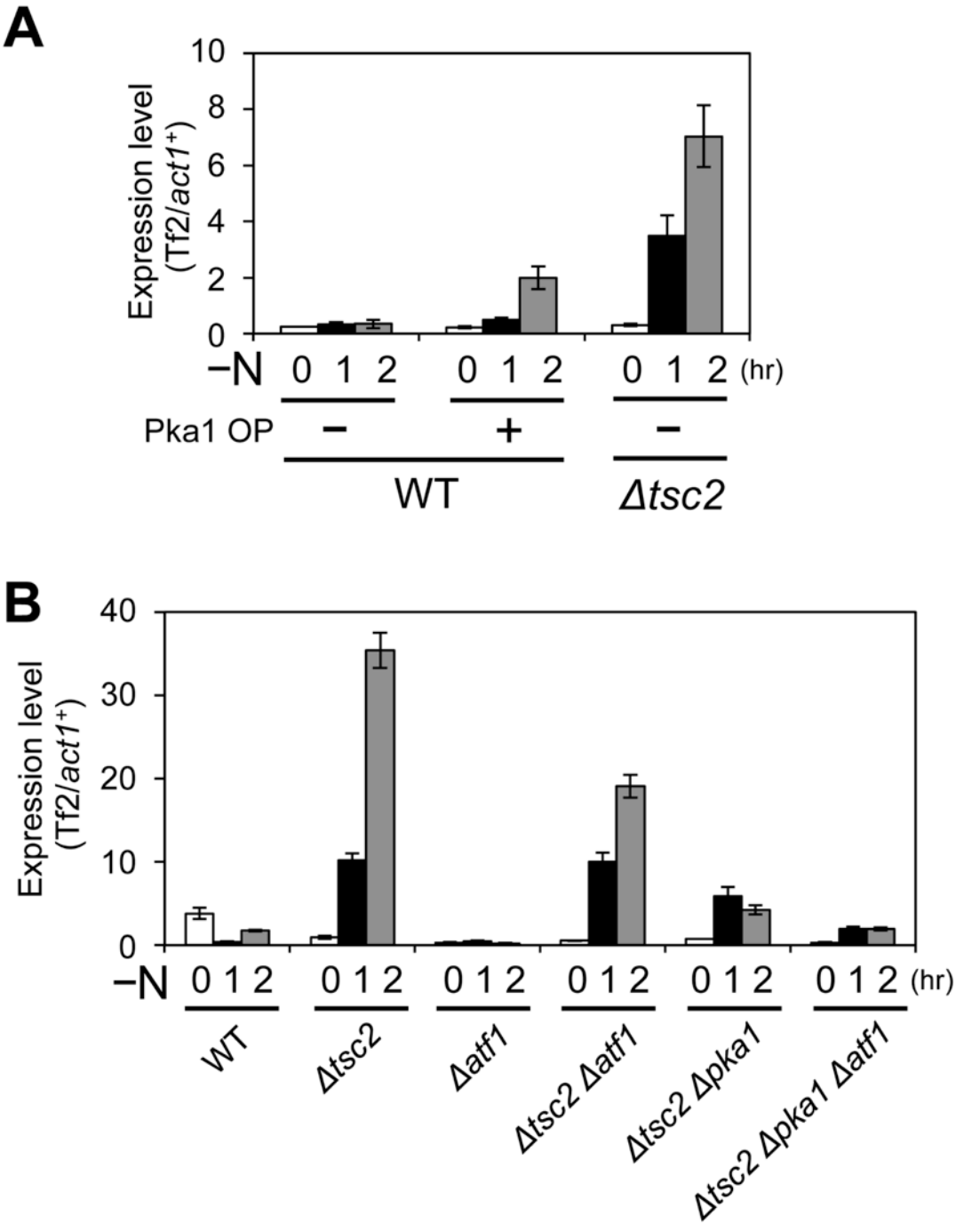

Figure S1. *Δatf1* partially suppresses *Tf2s* expression in *Δtsc2* cells.

(A) Overexpression of Pka1 in Wild-type slightly induces *Tf2*s expression after nitrogen starvation. Wild-type cells were transformed with pREP81 vector,

Journal of Cell Science • Supplementary information

plasmids expressing *pka1*$^{+}$. Transformants were grown to mid-log phase in nitrogen-rich medium containing thiamin (EMM+N+Thi) and then transferred to thiamin-free medium (EMM+N-Thi) and cultured for 22 hr. After that, cells were shifted to nitrogen-poor medium (EMM-N-Thi). Cells were treated and analyzed as in Fig. 1C.

(B) *Δatf1* suppresses *Tf2*s expression in *Δtsc2* mutant. Cells were treated and analyzed as in Fig. 1C.

Journal of Cell Science • Supplementary information

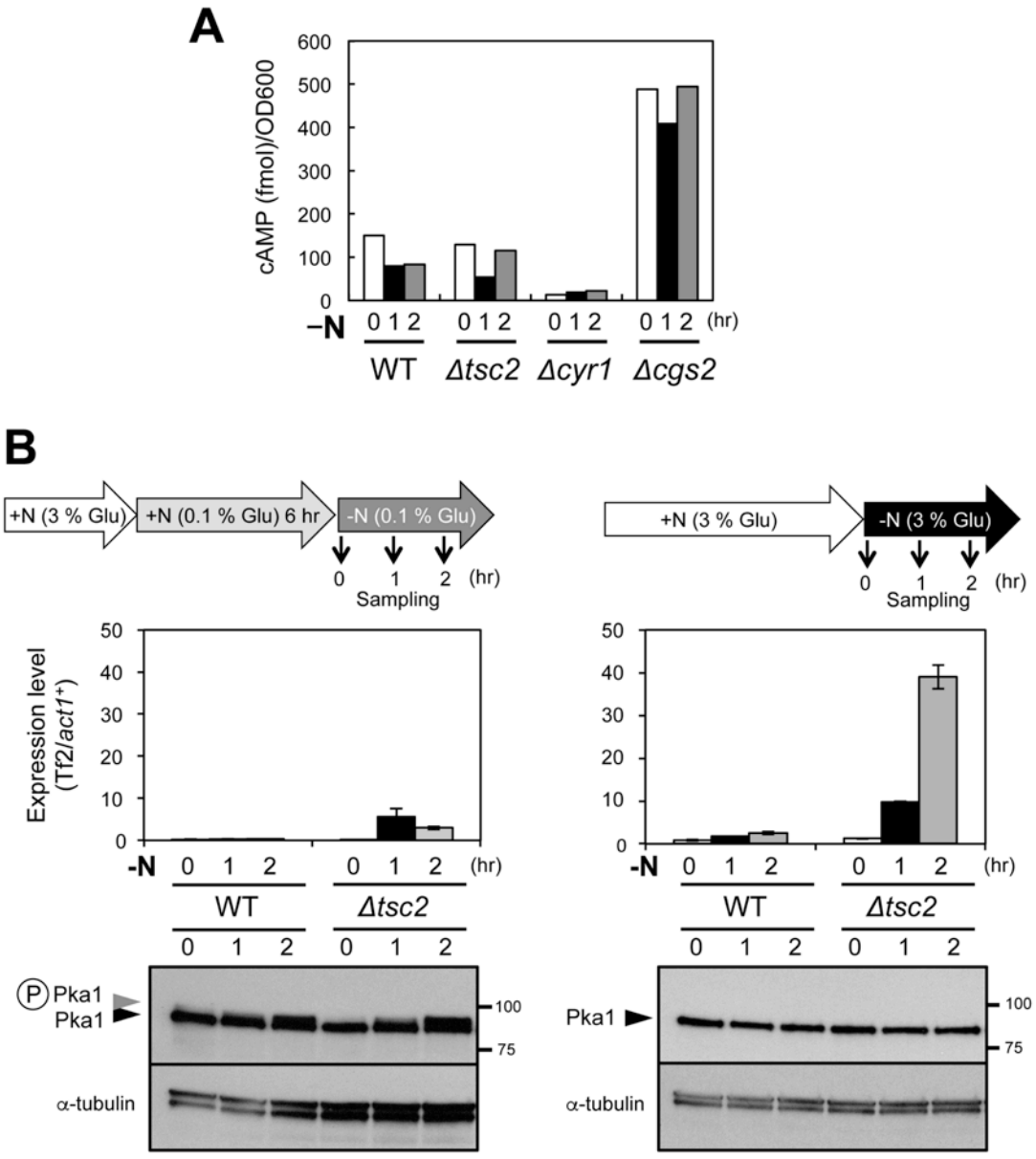

Figure S2. Glucose/cAMP signaling pathway in *Δtsc2*.

(A) Intracellular cAMP level in *Δtsc2* mutant strain. Each strain was precultured overnight in EMM (containing 3 % glucose) plus nitrogen and then transferred to EMM (contained 3 % glucose) minus nitrogen. Intracellular cAMP level was

Journal of Cell Science • Supplementary information

assayed using EIA system (Amarsham).

(B) Pka1 phosphorylation in *Δtsc2* mutant strain. Pka1 undergoes inhibitory phosphorylation under glucose starvation. Upper left and right figures show the schema of culture conditions. Each strain expressing Pka1-GFP was grown to mid-log phase in nitrogen-rich medium contained 3 % glucose and then transferred to glucose-depleted medium for 6 hr. After that, strain was shifted to nitrogen-poor and glucose-deplete medium (left). Each strain was grown to mid-log phase in nitrogen-rich medium contained 3 % glucose and then transferred to nitrogen-depleted medium (right). Middle left and right figures show qRT-PCR of *Tf2s* RNA levels. Lower left and right figures show western analysis of Pka1-GFP.

Journal of Cell Science • Supplementary information

Table S1. *S. pombe* strains used in this study

Strain	Genotype	Source
972h$^-$	*h$^-$*	(Matsumoto et al., 2002)
SP6	*h$^-$ leu1-32*	Matsumoto *et al*., (2002)
AE512	*h$^-$ tsc2::ura4$^+$ ura4-D18 leu1-32*	Matsumoto *et al*., (2002)
AE509	*h$^-$ tsc2::ura4$^+$ ura4-D18*	Matsumoto *et al*., (2002)
M5-2g3	*h$^-$ rhb1-DA4*	Murai *et al*., (2009)
M5-1e1	*h$^-$ rhb1-DA4 leu1-32*	Murai *et al*., (2009)
YKK280	*h$^+$ tor2^{ts10} tsc2::ura4$^+$ ura4-D18*	This study
YKK659	*h$^-$ tor2^{s65}*	This study
YKK884	*h$^+$ atg1::ura4$^+$ GFP-Tf2-13:kan^R ura4-D18*	This study
YKK888	*h$^+$ atg13::ura4$^+$ GFP-Tf2-13:kan^R ura4-D18*	This study
YKK141	*h$^+$ GFP-Tf2:kan^R*	This study
YKK140	*h$^+$ tsc2::ura4$^+$ GFP-Tf2-13:kan^R ura4-D18*	This study
DY11904	*h$^+$ CFP-atg8:leu1$^+$ leu1-32*	Sun *et al*., (2013)
YKK897	*h$^-$ tor2^{ts10} CFP-atg8:leu1$^+$ leu1-32*	This study
YKK903	*h$^-$ abp1::LEU2 CFP-atg8:leu1$^+$ leu1-32*	This study
YKK908	*h$^-$ tor2^{ts10} abp1::LEU2 CFP-atg8:leu1$^+$ leu1-32*	This study
YKK812	*h$^-$ abp1::LEU2 leu1-32*	This study
YKK899	*h$^-$ tsc2::ura4$^+$ CFP-atg8:leu1$^+$ leu1-32*	This study
DY11900	*h$^-$ atg1::kanMX CFP-atg8:leu1$^+$ leu1-32*	Sun *et al*., (2013)
YKK874	*h$^-$ tsc2::ura4$^+$ atg1::ura4$^+$ GFP-Tf2-13:kanR ura4*	This study
YKK1031	*h$^-$ tor2^{ts10} tsc2::ura4$^+$ CFP-atg8:leu1$^+$ leu1-32*	This study
YKK909	*h$^-$ atg1::kanMX GFP-Tf2-13:kan^R*	This study
YKK1058	*h$^-$ cpy-mCherry:kan^R GFP-Tf2-13:kan^R atg1::ura4$^+$ ura4-D18*	This study
YKK1059	*h$^-$ cpy-mCherry:kan^R GFP-Tf2-13:kan^R*	This study

FY7285	*h⁺ cyr1::ura4⁺ ura4-D18*	YGRC/NBRP
YKK158	*h⁺ cgs2::ura4⁺ ura4-D18*	This study
YKK424	*h⁺ tor1::ura4⁺ ura4-D18*	This study
YKK418	*h⁺ tsc2::ura4⁺ tor1::ura4⁺ ura4-D18*	This study
YKK77	*h⁻ tsc2::ura4⁺ cyr1::ura4⁺ ura4-D18 leu1-32*	This study
YKK230	*h⁻ tsc2::ura4⁺ pka1::ura4⁺ ura4-D18*	This study
YKK154	*h⁻ pka1::ura4⁺ ura4-D18*	This study
YKK155	*h⁻ pka1::ura4⁺ rhb1-DA4 ura4-D18*	This study
YKK1048	*h⁻ pka1::ura4⁺ ura4-D18*	This study
YKK1047	*h⁻ pka1::ura4⁺ atg1::ura4⁺ ura4-D18*	This study
YKK1052	*h⁻ cgs2::ura4⁺ atg1::ura4⁺ GFP-Tf2-13:kan^R ura4-D18*	This study
YKK1015	*h⁺ atf1::ura4⁺ GFP-Tf2-13:kan^R ura4-D18*	This study
YKK1070	*h⁻ tsc2::ura4⁺ atf1::ura4⁺ GFP-Tf2-13:kan^R ura4-D18*	This study
YKK1072	*h⁻ tsc2::ura4⁺ atf1::ura4⁺ pka1::ura4⁺ ura4-D18*	This study

Journal of Cell Science • Supplementary information